Int. J. Heat Mass Transfer. Vol. 10. pp. 61–81. Pergamon Press 1967. Printed in Great Britain

HEAT TRANSFER IN THE CONSTANT PROPERTY TURBULENT BOUNDARY LAYER

F. A. DVORAK and M. R. HEAD
Engineering Department, University of Cambridge

(*Received* 18 *April* 1966 *and in revised form* 13 *May* 1966)

Abstract—A new method has been developed for calculating heat transfer in the constant property turbulent boundary layer with arbitrary distributions of wall temperature and stream velocity. The procedure is as follows.

The development of the boundary layer is calculated by one or another of the methods currently available and from the calculated values of H and θ velocity profiles are specified by the use of a suitable two-parameter family. With the velocity distribution in the boundary layer completely determined, shear stress profiles are obtained by applying the equation of motion, and from the profiles of shear stress and mean velocity corresponding profiles of effective viscosity readily follow.

With some plausible assumption for turbulent Prandtl number the heat-transfer equation can then be solved directly by a digital computer to obtain temperature profiles and the heat transfer at the wall.

The method has been applied in zero and adverse pressure gradients with a step in wall temperature following an initial unheated entry length. Temperature profiles are well behaved and show a region of near similarity in the wall region as observed experimentally elsewhere. It is noticeable that in the adverse pressure gradient heat transfer falls off very much less rapidly than skin friction as separation is approached.

NOMENCLATURE

$A_1, A_2 \ldots$, matrix coefficients;
c, unheated entry length;
C_p, specific heat at constant pressure;
G, constant in matrix;
k, molecular conductivity;
k_t, eddy conductivity;
q, heat-transfer rate;
ρ, density;
T, temperature;
T_∞, undisturbed free-stream temperature;
T_w, local wall temperature;
τ, shear stress;
τ_w, local wall shear stress;
U, local velocity outside boundary layer;
U_∞, undisturbed free stream velocity;
x, y, rectangular coordinates along and normal to surface;
u, v, components of velocity in x- and y-directions;
δ, velocity boundary-layer thickness;
δ_T, thermal boundary-layer thickness;
δ^*, displacement thickness

$$= \int_0^y \left(1 - \frac{u}{U}\right) \mathrm{d}y \; ;$$

δ_s, boundary-layer thickness used by Sarnecki [13];
θ, momentum thickness

$$= \int_0^y \frac{u}{U}\left(1 - \frac{u}{U}\right) \mathrm{d}y \; ;$$

ν, kinematic viscosity;
ν_t, eddy viscosity;
α, thermal molecular diffusivity ($= k/\rho C_p$).

Dimensionless quantities

c_f, local skin friction coefficient ($= \tau_w/\frac{1}{2}\rho U^2$);
H, shape factor ($= \delta^*/\theta$);

$H_{\delta-\delta^*}$, shape factor suggested by Head $[= (\delta - \delta^*)/\theta]$;
Pr, laminar Prandtl number $(= \rho C_p \nu/k)$;
Pr_t, turbulent Prandtl number $(= \rho C_p \nu_t/k_t)$;
R_x, length Reynolds number $(= Ux/\nu)$;
R_θ, momentum thickness Reynolds number $(= U\theta/\nu)$;
R_c, Reynolds number at start of heating $(= Uc/\nu)$;
R, Reynolds number used by Hatton [3]

$$= \int_0^x \frac{U}{\nu}\,\mathrm{d}x \ ;$$

St, Stanton number $[= k(\partial T/\partial y)_w/\rho C_p U(T_w - T_\infty)]$;
U_τ, friction velocity $[= \sqrt{(\tau_w/\rho)}]$;
x^+, dimensionless distance along the wall

$$\left[= \int_0^R (c_f/2)^{\frac{1}{2}}\,\mathrm{d}R\right];$$

y^+, dimensionless distance normal to wall $(= U_\tau y/\nu)$;
Z, pressure gradient parameter used by Hatton [3] $[= (1/U)\,\mathrm{d}U/\mathrm{d}R]$;
t_*, reference temperature for wall law $[= k(\partial T/\partial y)_w/\rho C_p U_\tau]$;
t^+, dimensionless temperature $[= (T_w - T)/t_*]$;
P, term in general stability criterion $(= \alpha/U)$.

1. INTRODUCTION

TRADITIONALLY the subject of heat transfer from a solid surface to a fluid flowing over it is based on the correlation of experimental data by the use of suitable non-dimensional groups. This approach has been necessitated by the complexity of the phenomena involved and the general intractability of the problem particularly where internal flows are involved. By contrast the problems facing the aerodynamicist (at least until the advent of high-speed aircraft and missiles) have been relatively tractable and considerable progress has been made with the problem of calculating turbulent boundary-layer development for arbitrary distributions of external pressure and (more recently) of suction or blowing through the surface. The present paper is an attempt to make use of the advances that have been made along these lines to calculate heat transfer and the development of the temperature boundary layer, coupling the temperature and velocity fields by assumptions as to laminar and turbulent Prandtl numbers. This approach is not altogether new and follows on work which was initiated by Spalding [1] and carried on by Hatton [2, 3] and Patankar and Spalding [4].

The approach adopted here is the following: if the development of the turbulent boundary layer can be calculated with reasonable precision not only is the velocity field determined but also the distribution of shear stress throughout the layer. This in turn implies a distribution of effective viscosity which can be determined from the profiles of mean velocity and shear stress. Once the effective viscosity has been determined the effective conductivity follows from suitable assumptions for the laminar and turbulent Prandtl numbers. The heat-transfer equation can then be written in a suitable finite-difference form and solved by a digital computer to give temperature profiles and the heat transfer at the wall.

If the method of calculating boundary-layer development makes use of families of shear-stress profiles, or assumptions concerning eddy viscosity, then of course the general calculation procedure will be considerably shortened.

2. GENERAL OUTLINE OF CALCULATION PROCEDURE

The following lists the consecutive stages in the calculation of heat transfer for arbitrary distributions of wall temperature and external stream velocity. Constant fluid properties and two-dimensional flow are assumed.

(i) The development of the turbulent boundary layer is calculated by the use of the two-dimensional momentum integral equation, some relation (such as that due to Ludwieg and Tillmann [5]) expressing c_f as a function of R_θ and H and a suitable auxiliary equation.

(ii) With the development of R_θ and H known, a suitable two-parameter family of boundary-layer velocity profiles is used to specify the distribution of velocity through the boundary layer at suitably closely spaced intervals along the surface.

(iii) From the velocity profiles and the known distributions of skin friction and external velocity shear stress profiles are obtained by the use of the boundary-layer equation

$$u\frac{\partial u}{\partial x} + v\frac{\partial u}{\partial y} = U\frac{\mathrm{d}U}{\mathrm{d}x} + \frac{1}{\rho}\frac{\partial \tau}{\partial y}, \qquad (1)$$

i.e.

$$\tau_y = \tau_w - \rho\left[\int_0^y \left(U\frac{\mathrm{d}U}{\mathrm{d}x} - u\frac{\partial u}{\partial x} - v\frac{\partial u}{\partial y}\right)\mathrm{d}y\right]. \qquad (2)$$

(iv) From the profiles of shear stress and mean velocity, profiles of effective viscosity (i.e. $\nu + \nu_t$) follow.

(v) With laminar and turbulent Prandtl numbers known or assumed, profiles of effective conductivity (i.e. $k + k_t$) are obtained.

(vi) With the velocity field and distribution of effective conductivity defined, the heat-transfer equation is solved numerically for given boundary conditions [i.e. $T_w = T_w(x)$ or $q_w = q_w(x)$].

The accuracy of the final result will be limited by the accuracy of the initial boundary-layer calculation, by the accuracy with which the chosen family of velocity profiles represents the true distributions of velocity through the boundary layer and finally by the accuracy of the assumption for turbulent Prandtl number. These points are discussed further in the next section. It would seem that the above limitations must be inherent in any proposed calculation method and that the present procedure should give results which are in principle as accurate as can be achieved at the present stage. The numerical solution of the heat-transfer equation, once the distributions of mean velocity and effective conductivity have been specified, would appear from the present calculations to represent in most cases a comparatively negligible source of error.

3. DISCUSSION OF METHODS OF CALCULATING TURBULENT BOUNDARY-LAYER DEVELOPMENT, AND ASSUMPTIONS CONCERNING VELOCITY PROFILE FAMILIES AND TURBULENT PRANDTL NUMBER

3.1 *Calculation of the turbulent boundary layer*

It is generally accepted that the momentum integral equation in the form

$$\frac{\mathrm{d}\theta}{\mathrm{d}x} = \frac{c_f}{2} - (H+2)\frac{\theta}{U}\frac{\mathrm{d}U}{\mathrm{d}x} \qquad (3)$$

may be used with small error except close to separation where the neglected normal stresses due to turbulence become appreciable.

To use equation (3) it is necessary to have, in addition, a relationship of the form

$$c_f = c_f(R_\theta, H), \qquad (4)$$

and an auxiliary equation for the calculation of the form parameter H.

The first and best known skin friction relation of the form given by equation (4) is that due to Ludwieg and Tillmann [5], but more recent proposals have been made, and the relationship given by Thompson [6] in chart form has been used here because it is compatible with, and is in fact derived from, the family of profiles which we have used and which is discussed below.

A review of the various equations which have been proposed for the calculation of H has been given fairly recently by Thompson [7], and from this it appears that the entrainment equation due to Head [8] gives much better agreement with a wide range of experimental

data than do the earlier equations of Spence, Maskell, Truckenbrodt, etc. Thompson has in fact somewhat improved upon Head's original equation by (inter alia) incorporating a dependence of the non-dimensional rate of entrainment on $\theta\, dH/dx$. (In Head's original method, the non-dimensional rate of entrainment is assumed to be specified by the value of the form parameter $(\delta - \delta^*)/\theta$ which is in turn assumed to be uniquely related to the conventional form parameter H). Because Head's method was considerably simpler to use and a computer program for it already existed it has been employed in the present calculations. The general level of agreement with experiment is indicated by the two examples shown in Fig. 1. More recently proposed methods (see for example Escudier and Nicoll [9]. McDonald and Stoddart [10]) appear to offer no decisive advantages over that used here.

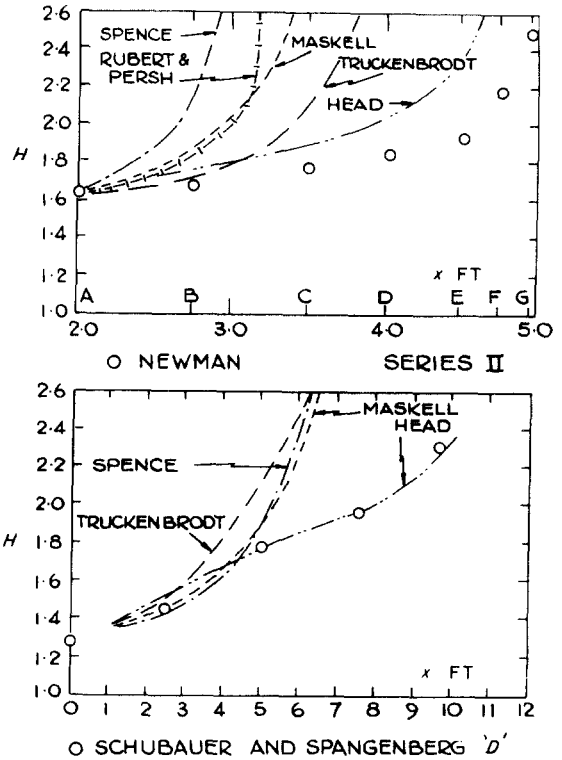

FIG. 1. Comparison of calculated shape factor developments (Figs. 17 and 19, reference [7]).

3.2 *Profile families*

In a wide variety of conditions the distribution of velocity in a region close to the wall can be described by the so-called universal law of the wall which takes the form

$$\frac{u}{U_\tau} = f\left(\frac{U_\tau y}{\nu}\right).$$

If the skin friction and the value of ν are known, the velocity distribution in the wall region is fixed (see Fig. 2); and if the stream velocity and boundary-layer thickness are also specified, the only problem in defining the velocity profile is to choose a plausible fairing such as that shown dotted in Fig. 2. Coles' [11] so-called wake law is perhaps the best known method of producing such a fairing and a two-parameter family of profiles can be built up by adding appropriate amounts of a universal wake function to the basic inner law profile. Coles' wake function can be conveniently approximated by a cosine function as noted by Spalding and better agreement with measurement may be obtained by incorporating the improvement suggested by Cornish [12].

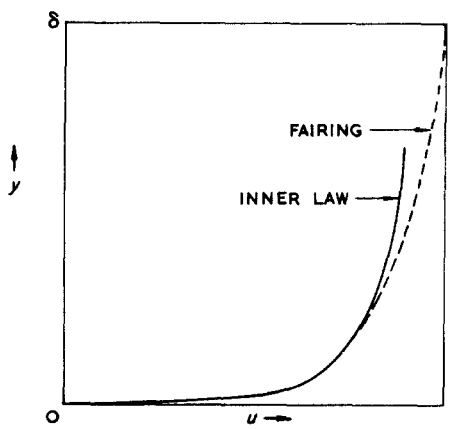

FIG. 2. Construction of two-parameter family of velocity profiles. Inner law curve fixed by values of τ and ν. Arbitrarily fixing values of δ and u with suitable fairing to inner law curve will then give H, R_θ and c_f.

A quite different approach has been suggested by Sarnecki [13]. He proposed that the velocity profile is the result of time sharing between turbulent and non-turbulent flow. By assuming that the velocity during time turbulent was given by the universal inner law extended through the layer and that the irrotational velocity was that of the free stream, he was able to obtain a universal distribution of intermittency which gave an excellent fit with measured profiles. This approach was used by Thompson [6] to produce a two-parameter family of profiles given explicitly in the form of charts, and a corresponding skin friction law. These have been used in the present calculations. Typical comparisons with measured profiles are shown in Figs. 3(a) and 3(b).

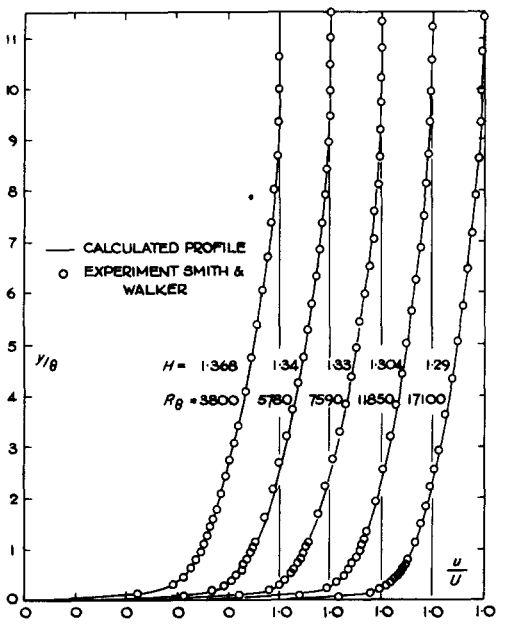

FIG. 3(a). Comparison of Thompson's family of mean velocity profiles with experiment (Fig. 9, reference [6]).

Profile families based on the use of the universal inner law will break down in sufficiently strong pressure gradients, either favourable or adverse (see, for example, reference [14]). The present calculations therefore cannot be expected to be accurate in the neighbourhood of separation.

3.3 *Turbulent Prandtl number*

Reynolds suggested that, because heat and momentum are transferred in turbulent flow by basically the same mechanism, the effective Prandtl number should be unity. This assumption has been widely made, but a survey of experimental data by Kestin and Richardson [15] suggests that, at least for air or other gases with a laminar Prandtl number near unity, a value of 0·8 should be more appropriate (see Fig. 4). It would in fact be expected that the turbulent Prandtl number should be less than unity in these circumstances since, due to pressure forces, a lump of fluid moving transverse to a gradient of velocity and temperature will come more rapidly into velocity equilibrium with its surroundings than into temperature equilibrium. The effective mixing length for momentum transfer will therefore be less than that for heat transfer, as Hinze [16] suggests, and heat will be more effectively transferred than momentum. Similar considerations may be applied to determine the probable effect of laminar conductivity on turbulent Prandtl number. A high laminar conductivity would be expected to reduce the transfer of heat by turbulent mixing, since a lump of fluid will tend to achieve temperature equilibrium with its surroundings more rapidly, so reducing the effective mixing length for heat. Thus it is to be expected that a low laminar Prandtl number will be associated with a high turbulent Prandtl number and conversely. These effects have been examined theoretically by Saffman [17], and Mizushina and Sasano [18] have carried out experiments in which it was found that, to obtain agreement with measured heat transfer in the case of liquid metals (low laminar Prandtl number), it was necessary to assume a high turbulent Prandtl number in the region of the wall. Present calculations have been restricted to turbulent Prandtl numbers of 1·0 and 0·8.

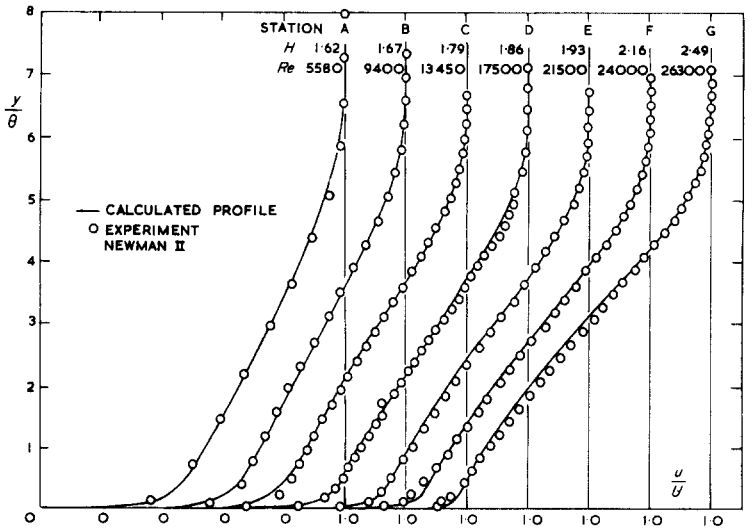

FIG. 3(b). Comparison of Thompson's family of mean velocity profiles with experiment (Fig. 12, reference [6]).

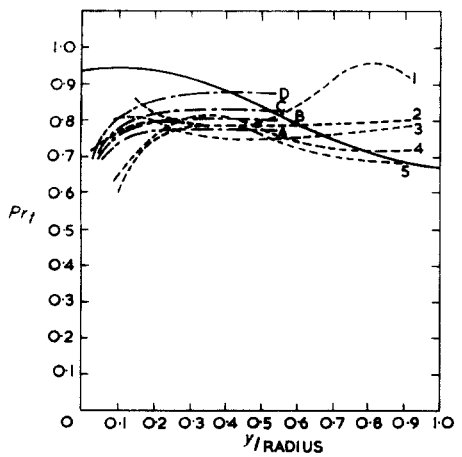

FIG. 4. Variation of turbulent Prandtl number Pr_t with distance from wall (Fig. 11, reference [15]).

4. CASES TREATED

The general case considered is that of a turbulent boundary layer developing in zero pressure gradient and with zero heat transfer up to a point where there is a step increase in wall temperature. Beyond this point either the zero pressure gradient condition is maintained or the velocity outside the boundary layer decreases linearly as shown in Fig. 5.

At the discontinuity in wall temperature, which forms the starting point of the present calculations, it is assumed that

$$Re = 1{\cdot}15 \times 10^6$$
$$H = 1{\cdot}41$$
$$Re_\theta = 2690.$$

The values of Re_θ and H are approximately those given by Coles for the flat plate Reynolds number chosen (see Table II 3 of Thwaites, [19]).

With these starting values the subsequent development of velocity and temperature boundary layers has been calculated:

(1) for zero pressure gradient and
  (a) $Pr = 0{\cdot}7\ Pr_t = 1{\cdot}0$
  (b) $Pr = 0{\cdot}01\ Pr_t = 1{\cdot}0$
  (c) $Pr = 10{\cdot}0\ Pr_t = 1{\cdot}0$

(2) for adverse pressure gradient and
  (a) $Pr = 0{\cdot}7\ Pr_t = 1{\cdot}0$
  (b) $Pr = 0{\cdot}7\ Pr_t = 0{\cdot}8$.

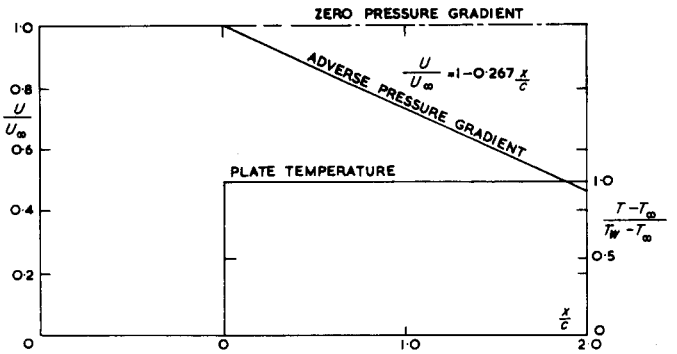

FIG. 5. Cases treated in calculations.

The work is continuing and it is intended to cover a further range of conditions.

5. DETAILS OF CALCULATIONS

A computer program already existed for calculating boundary-layer development. This was based on solving the momentum integral equation with analytic approximations to the curves of $c_f(R_\theta, H)$ given by Thompson, and to the curves of functions F and G used by Head for the simultaneous calculation of H. This program was used to calculate the developments of H, R_θ and c_f shown in Fig. 6 for zero and adverse pressure gradients.

Velocity profiles through the boundary layer were initially obtained using Thompson's charts, in which u/U is presented as $u/U(y/\theta, H, R_\theta)$. As taken from the charts, however, the profiles were scarcely accurate enough for the present purpose. If the actual values of

$$\int_0^{\delta/\theta} \frac{u}{U}\left(1 - \frac{u}{U}\right) \mathrm{d}(y/\theta)$$

for the profiles were not accurately equal to unity, or if the values of H and c_f were not those specified, then the shear-stress profiles obtained from them by the use of the momentum equation would not tend to zero at the boundary-layer edge. It was therefore found necessary to revert to the method which Thompson had used to build up his family of velocity profiles to obtain individual profiles with precisely the required characteristics (i.e. H and θ). A computer program was written for this purpose. Figs. 7 and 8 show representative profiles for zero and adverse pressure gradients.

A program due to McQuaid [20] already existed for determining shear stress profiles once velocity profiles and skin friction distribution were known, and this was used with minor modifications to obtain the profiles shown in Figs. 9 and 10.

Shear stress profiles and velocity profiles then gave profiles of effective viscosity and hence of eddy viscosity, ν_t, shown in Figs. 11 and 12. Some systematic irregularities in these curves will be noted; these could readily have been faired out but in fact the curves were used as they are shown since the irregularities appeared to have a negligible effect on the final temperature profiles.

With assumed laminar and turbulent Prandtl numbers the effective conductivity field was now known and this, along with the known distribution of mean velocity, enabled the heat-transfer equation to be solved by finite difference methods.

Following most earlier work in the subject Schmidt's [21] step-by-step difference (i.e. explicit) method was initially used. This proved satisfactory and enabled solutions to be obtained but at the cost of considerable computing time. To represent accurately conditions in the

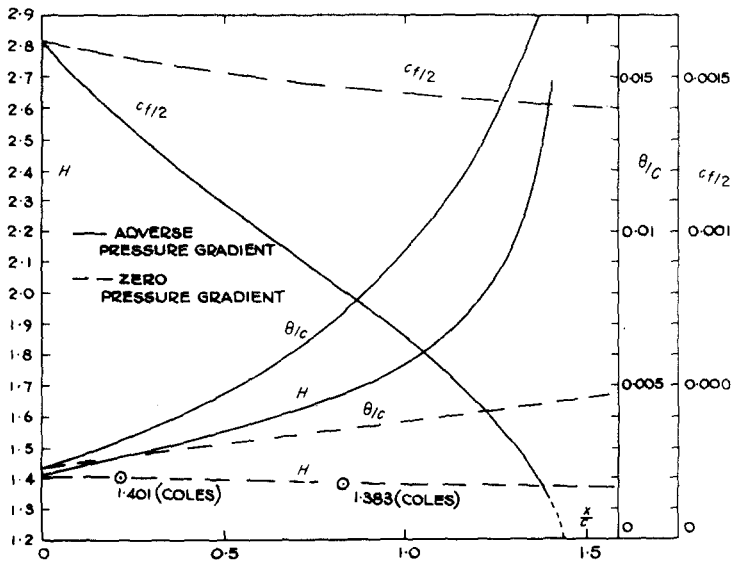

FIG. 6. Calculated developments of H, θ and $C_f/2$ for adverse and zero pressure gradients.

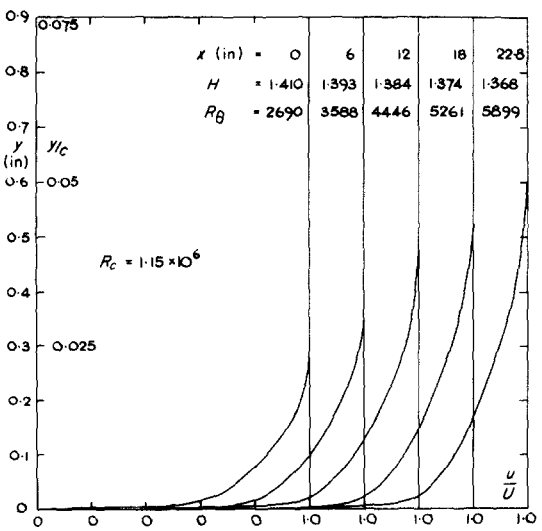

FIG. 7. Zero pressure gradient velocity profiles.

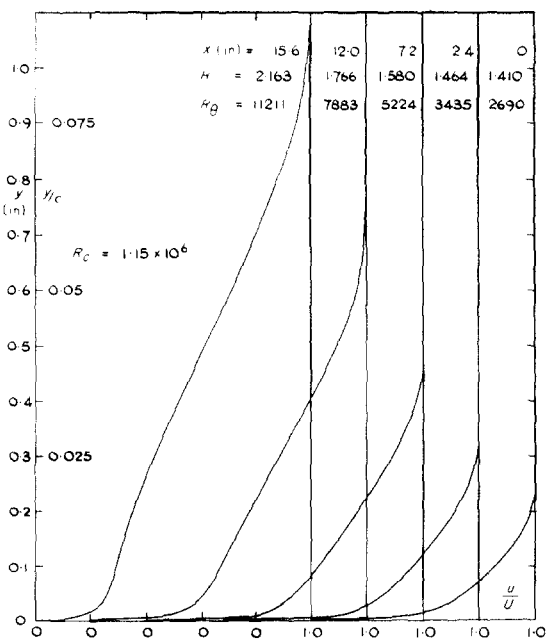

FIG. 8. Adverse pressure gradient velocity profiles.

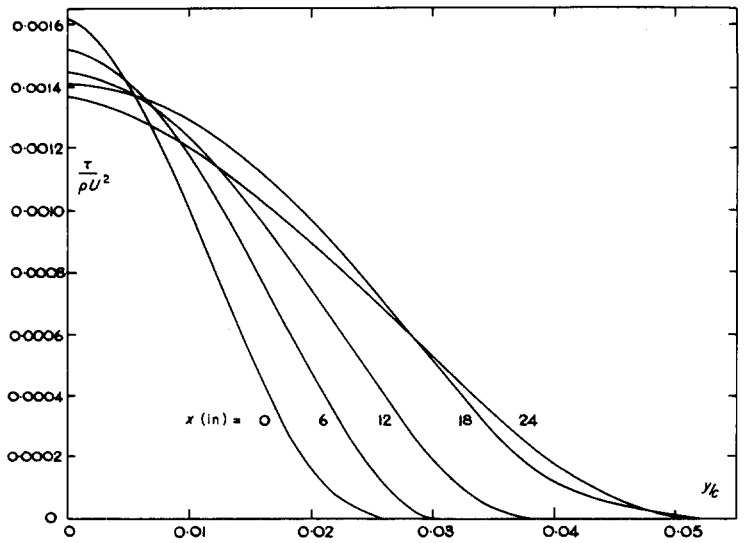

FIG. 9. Zero pressure gradient shear stress profiles.

immediate neighbourhood of the surface it was necessary to take very small steps in the y-direction (i.e. normal to the surface) and to keep the calculation stable it was then found necessary to take very small steps in the x-direction (i.e. along the surface). Typically, with 90 points taken through the boundary-layer thickness, values of y/c close to the surface were in the region of 0·0001 and corresponding values of x/c were approximately 0·0002.

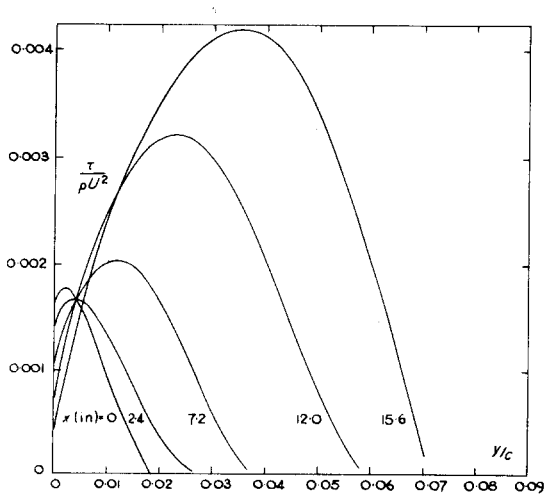

FIG. 10. Adverse pressure gradient shear stress profiles.

As a check on the accuracy of computation the integral of the heat flux through the surface to any particular point x was compared with the convective heat flux in the boundary layer at that point, i.e.

$$\int_0^x -k\left(\frac{\partial T}{\partial y}\right)_w \mathrm{d}x$$

was compared with

$$\int_0^{\theta_T} \rho C_p u\,(T_w - T)\,\mathrm{d}y.$$

In general the agreement was within 2·0 per cent.

Having shown that it was possible to obtain satisfactorily accurate solutions for both zero and adverse pressure gradients (at least up to fairly close to separation in the latter case) it was decided to try an alternative finite difference procedure for solving the heat-transfer equation. This was the Crank–Nicholson method [22] which is outlined in the Appendix along with the procedure initially used. The Crank–Nicholson method involves at each step in x the solution of n simultaneous equations where n is the number of points through the boundary-layer thickness. The time per step is therefore

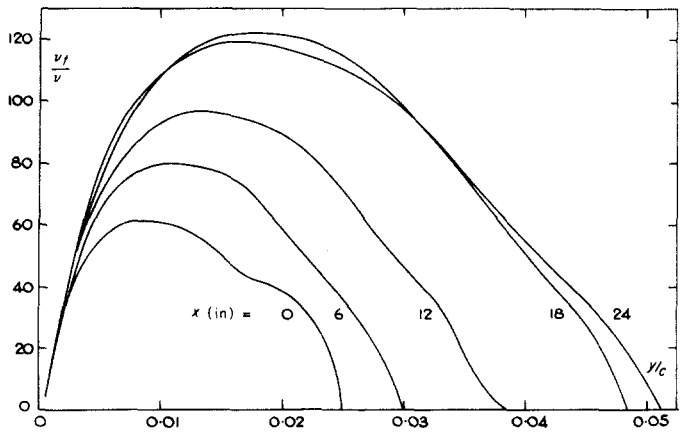

FIG. 11. Zero pressure gradient eddy viscosity profiles.

generally considerably longer than with the alternative explicit approach; the saving in computer time comes, however, through the ability to take very much longer steps (of the order of fifty times greater than with the explicit method) since there is no rigorous stability criterion to be satisfied. Where it is necessary for the sake of accuracy to take very short steps, as at the beginning of the heat-transfer region, no advantage is to be gained by the use of the Crank–Nicholson method and the procedure finally adopted as being most economical of computing time was to use the explicit method for the initial part of the calculation, then to change over to the Crank–Nicholson method. By this means the overall computing time was cut to about one twentieth of its previous value. The total computing time taken to complete a calculation, i.e. boundary-layer development, velocity, shear stress and eddy viscosity profiles and finally temperature profiles and heat-transfer rates for Case 2(a) (Section 4) was approximately 6 min on the Cambridge University Titan (Atlas II) Computer.

Cases 1(c) and 2(b) were treated by the explicit method, Case 1(b) by the Crank–Nicholson

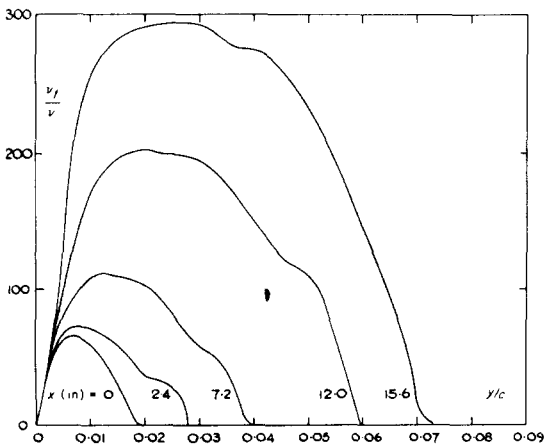

FIG. 12. Adverse pressure gradient eddy viscosity profiles.

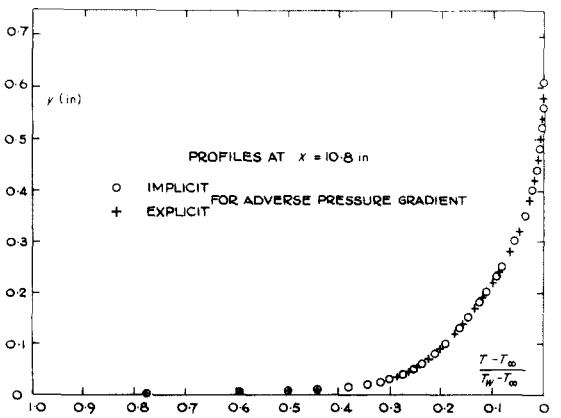

FIG. 13. Typical comparison of temperature profiles calculated by the explicit and implicit methods.

method only, Case 2(a) by both explicit and Crank–Nicholson methods and Cases 1(a), 2(a) and 1(c) by the combination of the two methods finally evolved. Where different methods were used the results obtained were generally in excellent agreement, a typical comparison of temperature profiles being shown in Fig. 13. In the case of 1(c) some discrepancy in the heat balance was noted when the Crank–Nicholson method was used, though values of $k(\partial T/\partial y)_w$ were virtually unaltered.

6. RESULTS AND DISCUSSION

6.1 *Calculations of boundary-layer development*

The development of the velocity boundary layer in zero pressure gradient follows very accurately that given by Coles, as the ringed points on Fig. 6 show. No such direct check is possible in the adverse pressure gradient case but the shear stress profiles and profiles of eddy viscosity shown in Figs. 9–12 are qualitatively very similar to those presented by Bradshaw and Ferriss [23] and other authors.

6.2 *Temperature profiles*

Calculated temperature profiles for air in zero pressure gradient, with Pr_t assumed equal to unity, are shown in Figs. 14, 15 and 16. In Fig. 14, which is a dimensionless plot on a log–log scale, three calculated profiles are compared with the universal profile suggested by Deissler [24]. It will be seen that the three sets of calculated points fall closely on a single curve which is in fair agreement with Deissler's. This single curve is compared in Fig. 15 on a semi-log plot with the measurements of Brundrett *et al.* [25] and Reynolds *et al.* [26]. The agreement here is very satisfactory and supports the suggestion that, at least in zero pressure gradient, there is a law of the wall for temperature analogous to that for velocity.

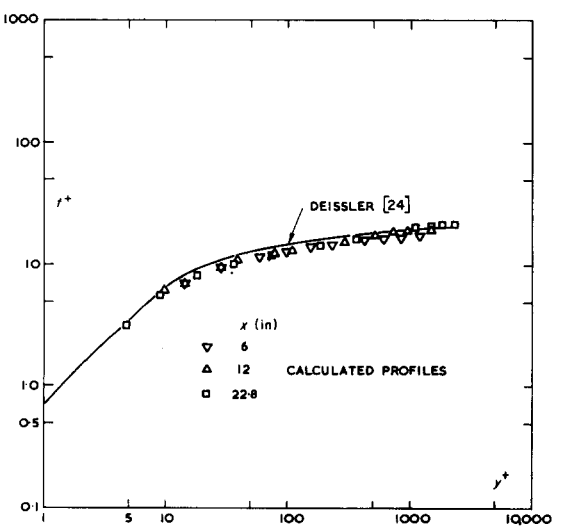

FIG. 14. Universal flat plate temperature profile for a fluid Prandtl number of 0·7.

Figure 16 shows a natural plot of the calculated temperature profiles for zero pressure gradient which may be compared with the temperature profiles calculated for the adverse pressure gradient case shown in Fig. 17. It will be seen that the adverse gradient has a quite marked effect on the general form of the temperature distribution through the layer.

Figure 18 shows the calculated temperature profiles for adverse pressure gradient plotted on a log–log scale and again compared with Deissler's curve. It will be seen that up to $x = 12$ in, where $H = 1{\cdot}766$, the agreement is not noticeably worse than for zero pressure gradient, but as separation is approached there is a very much greater divergence.

The effect of the assumption for turbulent Prandtl number (whether 0·8 or 1·0) on the form of the calculated temperature profile is shown in Fig. 19 along with the velocity profile at the same position. There is evidently a small but appreciable effect, the lower turbulent Prandtl number corresponding, as would be expected, to the greater thermal boundary-layer thickness.

Figure 20 shows the effect on the temperature profile of varying the laminar (or molecular) Prandtl number for a fixed turbulent Prandtl number of unity. In Section 3.3 it was indicated that there should be some effect of the laminar on the turbulent Prandtl number but the fact that this has been ignored should not affect the marked qualitative differences in profile shape

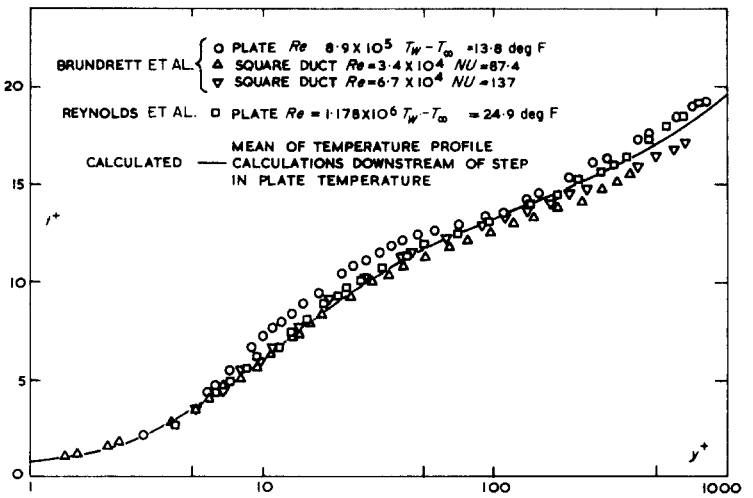

FIG. 15. Comparison between measured and calculated flat plate temperature profiles.

which are evident in Fig. 20. It will be seen that for a Prandtl number of 0·01 the temperature profile closely approaches the laminar form.

In Fig. 21 the developments of velocity and thermal boundary layers are compared for adverse and zero pressure gradients, the boundary-layer thicknesses being arbitrarily defined as the distances from the surface for which $u/U = 0{\cdot}999$ or $(T - T_\infty)/(T_w - T_\infty) = 0{\cdot}001$; the laminar Prandtl number here is 0·7 and the turbulent Prandtl number is taken as unity.

Figure 22 shows the effect of laminar Prandtl number on the growth of the thermal boundary layer; in particular it shows how, for a suffi-

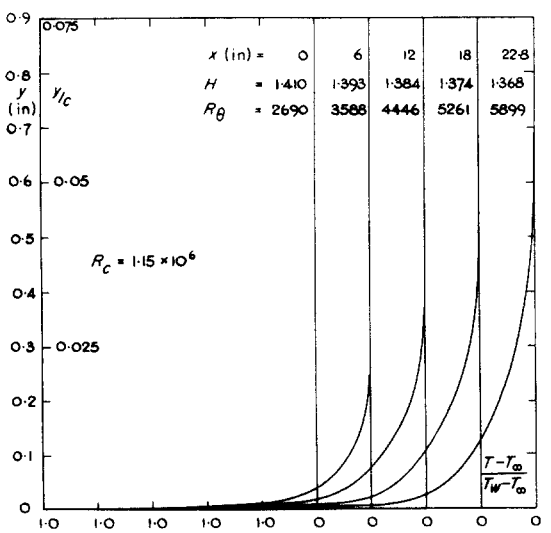

FIG. 16. Zero pressure gradient temperature profiles.

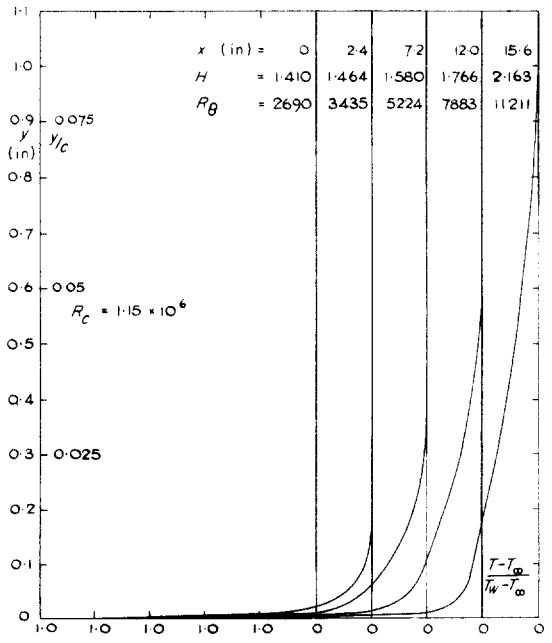

FIG. 17. Adverse pressure gradient temperature profiles.

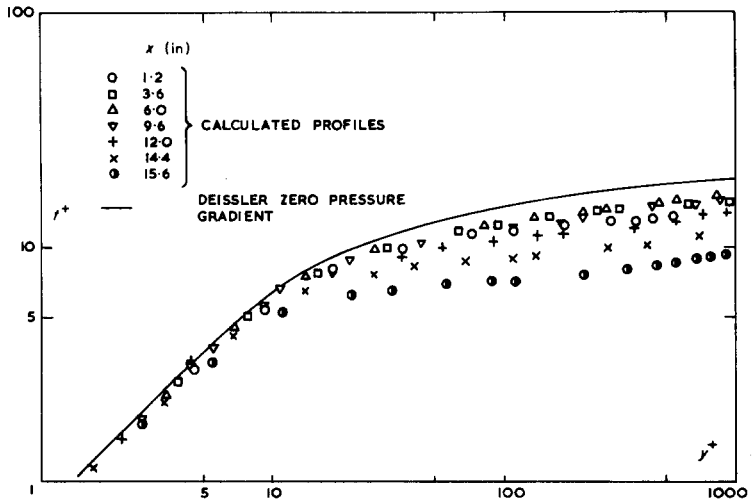

FIG. 18. Adverse pressure gradient temperature profiles.

ciently low Prandtl number, the thermal boundary layer rapidly extends beyond the edge of the velocity boundary layer. It will be noted that if a different measure of thermal boundary-layer thickness, notably

$$\int_0^\infty (T - T_\infty)/(T_w - T_\infty)\,dy,$$

had been used the effect of Prandtl number on rate of growth would have been very much more marked.

6.3 *Heat transfer*

The results of the present calculations for zero pressure gradient are shown in Fig. 23 compared with those of other authors. It will

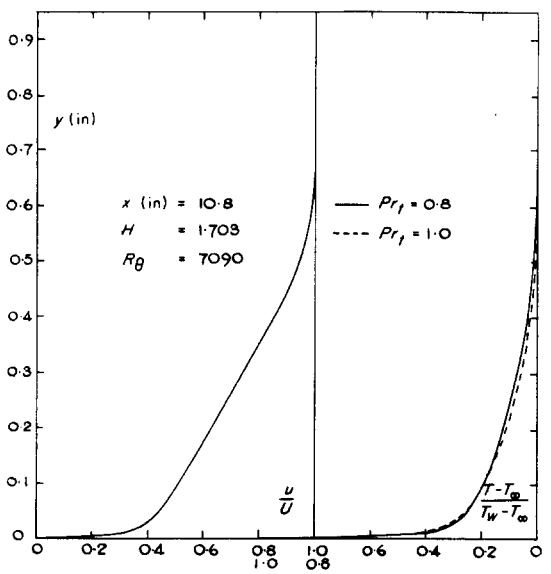

FIG. 19. Effect of assumed turbulent Prandtl number on temperature profiles in adverse pressure gradient.

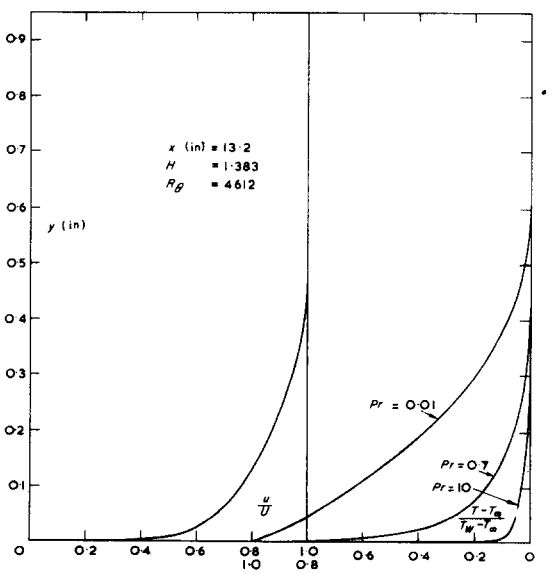

FIG. 20. Effect of laminar Prandtl number on temperature profiles in zero pressure gradient.

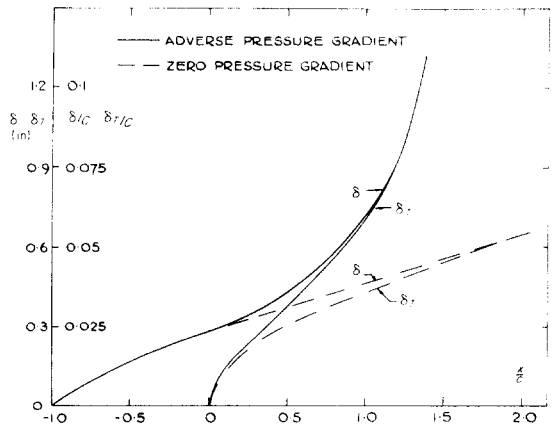

FIG. 21. Effect of pressure gradient on growth of velocity and thermal boundary layers.

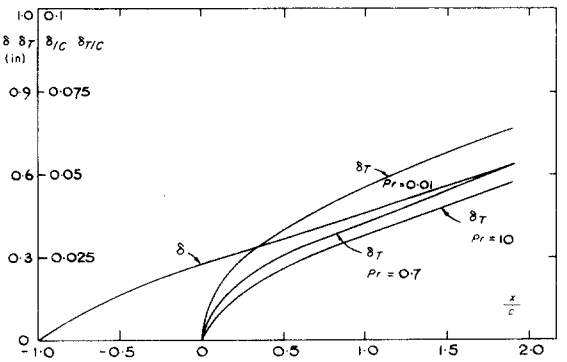

FIG. 22. Effect of laminar Prandtl number on growth of thermal boundary layer.

be seen that for a Prandtl number of 0·7 they are in remarkably good agreement at some little distance downstream of the beginning of heating, confirming both the validity of the approximations made in the earlier analyses and the accuracy of the present numerical approach. The result also confirms that the use of the dimensionless group $St\ Pr/(c_f/2)^{\frac{1}{2}}$ takes fair account of conditions near the start of heating, as was suggested by Spalding [1].

In the case where $Pr = 10$ there is a considerable difference between Hatton's results and those of the present authors. This is almost

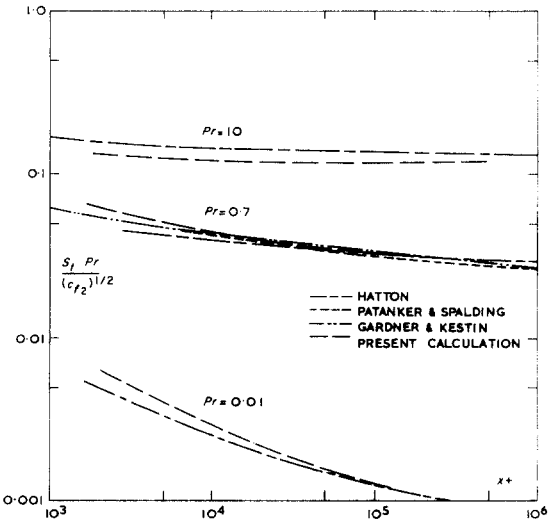

FIG. 23. Comparison of present heat-transfer results with those of other authors.

certainly due to the different forms used for the law of the wall in the sublayer region. In the present calculation it has been assumed, following Thompson, that

$$\text{for } y^+ < 8, \quad u^+ = y^+,$$

$$\text{and for } y^+ > 8, \quad u^+ = 5{\cdot}4 + 2{\cdot}3886 \ln (y^+ - 5{\cdot}03).$$

If the shear stress is substantially constant in the immediate vicinity of the wall, as it is in zero pressure gradient, this implies that ν_t (and hence k_t) should be substantially zero for $y^+ < 8$. The expressions used by Hatton and Gardener and Kestin, however, imply ν_t (and hence k_t) $= 0$ only at the wall itself, so that in general they will predict higher values of heat transfer and the difference will be most marked where the laminar conductivity is low (i.e. at high Prandtl numbers). In these circumstances it is evidently important that the velocity distribution in the sublayer and blending region should be specified with considerable accuracy, and it seems likely that the approximation used here should lead to some error.

The disagreement between Hatton's and the present result for $Pr = 0{\cdot}01$ is similar to that

observed for $Pr = 0{\cdot}7$ and may be due to the present starting conditions, since the results run together sufficiently far downstream.

Figure 24 shows the effect of adverse pressure gradient on the heat transfer. It will be seen that there is a marked reduction as compared with zero pressure gradient, though the temperature gradient at the wall does not fall off as rapidly as does the skin friction. In fact, close to separation the calculations show a rise in heat transfer. Intuitively, this does not seem altogether plausible, though it may be accounted for by the rapid rise in eddy viscosity (see Fig. 12), and hence of eddy conductivity, as separation is approached. The calculation in this region must, however, be viewed with some reserve; first because the law of the wall cannot be expected to hold with acceptable accuracy in the vicinity of separation, and second because the overall heat balance, which up to $x/c = 1{\cdot}2$ checks to within 2 per cent, becomes progressively less accurate as separation is approached. The reason for the inaccuracy of the calculation method in this region has not yet been found.

Figure 25 is a plot of the heat-transfer results in terms of Stanton number. This reduces considerably the difference between zero and adverse pressure gradient results, though the latter are still appreciably lower except close to separation. The effect of changing the turbulent Prandtl number from 1·0 to 0·8 is also shown, this giving as might be expected an increased rate of heat transfer in both zero and adverse pressure gradients.

The present heat-transfer results are in disagreement with those given by Hatton [3], insofar as they show that an adverse pressure gradient reduces the rate of heat transfer (except possibly close to separation) whereas Hatton's results show an increase. However, Hatton's results are almost certainly in error here since his assumption of a universal velocity profile (in terms of u^+ vs. y^+), whilst being quite reasonably satisfactory in zero pressure gradient, can give only a poor representation of the velocity profiles encountered in adverse pressure gradients. This is exemplified in Fig. 26 where Deissler's profile is compared both on the basis of equal skin friction and equal boundary-layer thickness with a typical adverse pressure gradient velocity profile. This was obtained from Thompson's charts, which the earlier comparisons with experiment [see Fig. 3(b)] have indicated should give a very good indication of overall profile shape. With Fig.

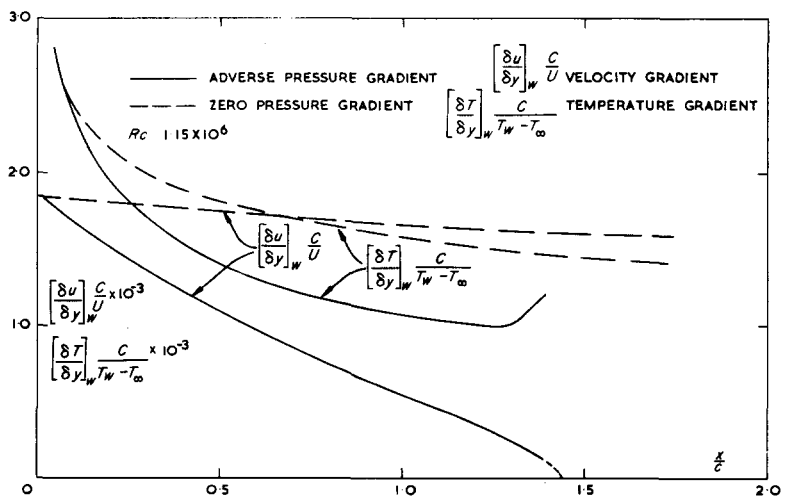

FIG. 24. Effect of adverse pressure gradient on heat transfer.

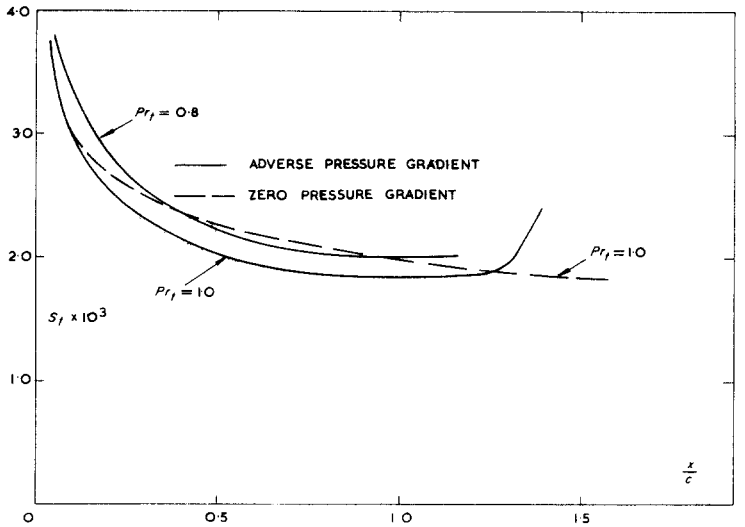

FIG. 25. Effect of turbulent Prandtl number on heat transfer.

26 in view it is not surprising that Hatton's heat-transfer results should be somewhat in error. What is perhaps surprising is that the quite severe adverse pressure gradient assumed in the present calculations should have the relatively small effect on heat transfer indicated in Fig. 25. It is evident that the effect of the rapidly increasing eddy conductivity and boundary-layer thickness as separation is approached largely offsets, if it does not actually exceed, the effect of applying the straightforward Reynolds analogy at the wall.

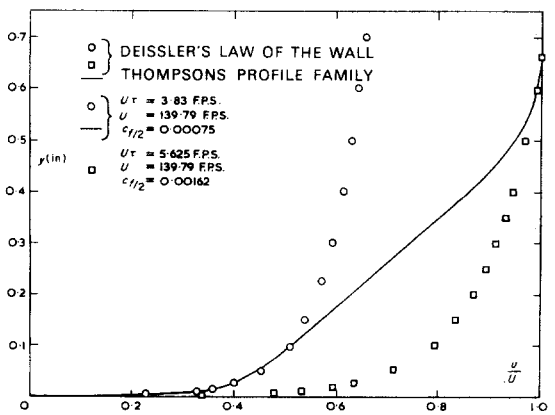

FIG. 26. Comparison of typical adverse pressure gradient profile with profile used by Hatton.

7. CONCLUSIONS

From the present investigation it is concluded that:

(i) by the use of suitable computer programs plausible profiles of shear stress and eddy viscosity can be determined from calculated boundary-layer development and an assumed two-parameter family of velocity profiles;

(ii) with the mean velocity field known and distributions of effective conductivity obtained from a knowledge of the eddy viscosity and assumed laminar and turbulent Prandtl numbers temperature profiles and the heat-transfer rate can be accurately determined;

(iii) considerable savings in computer time may be achieved by the judicious combination of explicit and implicit finite difference schemes for the solution of the heat-transfer equation;

(iv) the balance between heat transferred at the wall and that convected downstream provides a useful check on the numerical accuracy of the solution of the heat-transfer equation;

(v) the temperature distribution in the wall region conforms closely to a universal form for

zero pressure gradient and in adverse pressure gradients at least up to an value of 1·8;

(vi) the value chosen for the turbulent Prandtl number (whether 0·8 or 1·0) has a significant effect on the temperature profiles and heat transfer. From physical considerations and the experimental evidence collected by Kestin and Richardson [15] the value of 0·8 would appear to be the more suitable choice though 1·0 has been used here to facilitate comparison with other authors' results;

(vii) in zero pressure gradient the results are in broad agreement with those obtained elsewhere;

(viii) for sufficiently low laminar Prandtl numbers the heat transfer is greatly increased, the temperature boundary layer is considerably thicker than the velocity boundary layer and the temperature profile has a typically laminar appearance;

(ix) in an adverse pressure gradient the heat transfer at the wall falls off, but less rapidly than the skin friction, as separation is approached. The present results indicate an increase in the immediate vicinity of separation but the calculation may be somewhat in error in this region;

(x) the present results for adverse pressure gradient should be considerably more accurate than those obtained by assuming a universal form of velocity profile.

ACKNOWLEDGEMENT

The authors are indebted to Dr. A. P. Hatton for introducing them to the problem treated here and for helpful discussions.

REFERENCES

1. D. B. SPALDING, Heat transfer to a turbulent stream from a surface with a step-wise discontinuity in wall temperature, *Int. Dev. Heat Transfer*, ASME 439 (1961).
2. A. P. HATTON, Heat transfer through the turbulent incompressible boundary layer on a flat plate, *Int. J. Heat Mass Transfer* **7**, 875 (1964).
3. A. P. HATTON, Heat transfer through the incompressible boundary layer in the presence of moderate pressure gradient, *Int. J. Heat Mass Transfer* **8**, 1469 (1965).
4. S. V. PATANKAR and D. B. SPALDING, A calculation procedure for heat transfer by forced convection through two dimensional uniform-property turbulent boundary layers on smooth impermeable walls, Mech. Engng Dept. Imperial College, TWF/TN/7 (1965).
5. H. LUDWIEG and W. TILLMANN, Investigations of the wall shearing stress in turbulent boundary layers, NACA TM 1285 (1950).
6. B. G. J. THOMPSON, A new two-parameter family of mean velocity profiles for incompressible turbulent boundary layers on smooth walls, *Aero. Res. Coun.* 26830, F.M.3588 (1965).
7. B. G. J. THOMPSON, A critical review of existing methods of calculating the turbulent boundary layer, *Aero. Res. Coun.* 26109, F.M.3492 (1964).
8. M. R. HEAD, Entrainment in the turbulent boundary layer, *Aero. Res. Coun.* R. & M. 3152 (1958).
9. M. P. ESCUDIER and W. B. NICOLL, The entrainment function in turbulent boundary-layer and wall-jet calculations, Mech. Engng Dept., Imperial College TWF/R/1 (1965).
10. H. MCDONALD and J. A. P. STODDART, On the development of the incompressible turbulent boundary layer, B.A.C. Rep. Ae 225 (1965).
11. D. E. COLES, The law of the wake in the turbulent boundary layer, *J. Fluid Mech.* **1**, 191 (1965).
12. J. J. CORNISH, A universal description of turbulent boundary-layer profiles with or without transfiguration, Mississippi State University, Aerophysics Dept. Rep. no. 29 (1960).
13. A. J. SARNECKI, Ph.D. Dissertation, Cambridge University (1959).
14. V. C. PATEL, Calibrations of the Preston tube and limitations on its use in pressure gradients, *J. Fluid Mech.* **23**, 185 (1965).
15. J. KESTIN and P. D. RICHARDSON, Heat transfer across turbulent incompressible boundary layers, *Int. J. Heat Mass Transfer* **6**, 289 (1963).
16. J. O. HINZE, *Turbulence; an Introduction to its Mechanism and Theory*. McGraw-Hill, New York (1959).
17. P. G. SAFFMAN, On the effect of the molecular diffusivity in turbulent diffusion, *J. Fluid Mech.* **8**, 273 (1960).
18. T. MIZUSHINA and T. SASANO, The ratio of the eddy diffusivities for heat and momentum and its effect on liquid metal heat-transfer coefficients, *Int. Dev. Heat Transfer*, ASME, 662 (1961).
19. B. THWAITES, *Incompressible Aerodynamics*. Oxford University Press (1960).
20. J. MCQUAID, Private communication, Cambridge University Engineering Department (1965).
21. E. SCHMIDT, *Thermodynamics*, translated by J. KESTIN, Clarendon Press, Oxford (1949).
22. J. CRANK and P. NICHOLSON, A pratical method for numerical evaluation of solutions of partial-differential equations of the heat-conduction type, *Proc. Camb. phil. Soc. math. phys. Sci.* **43**, 50 (1947).
23. P. BRADSHAW and D. H. FERRISS, The response of a retarded equilibrium turbulent boundary layer and the sudden removal of pressure gradient, *Aero. Res. Coun.* 26758, F.M.3577 (1965).
24. R. G. DEISSLER, Analysis of turbulent heat transfer, mass transfer and friction in smooth tubes at high Prandtl and Schmidt number, NACA TN 3145 (1954); also NACA Rep. 1210 (1955).

25. E. BRUNDRETT, W. D. BAINES, J. PEREGRYM, and P. R. BURROUGHS, Inner and outer law descriptions of temperature and velocity in two- and three-dimensional boundary layers, AGARDograph 97, Part 2, 855 (1965).
26. W. C. REYNOLDS, W. M. KAYS and S. J. KLINE, Heat transfer in the turbulent incompressible boundary layer I—Constant wall temperature. NASA Tech. Mem. 12-1-58W (1958).
27. G. O. GARDNER and J. KESTIN, Calculation of the Spalding function over a range of Prandtl numbers. *Int. J. Heat Mass Transfer* **6**, 289 (1963).

APPENDIX

1. *Explicit method*

The heat transfer equation is

$$\rho C_p\left(u\frac{\partial T}{\partial x}+v\frac{\partial T}{\partial y}\right)=(k+k_t)\frac{\partial^2 T}{\partial y^2}+\frac{\partial k_t}{\partial y}\frac{\partial T}{\partial y} \tag{5}$$

with the boundary conditions

$$\begin{aligned} T &= T_\infty \quad \text{at} \quad x = 0 \quad \text{and all} \quad y > 0 \\ T &= T_\infty \quad \text{at} \quad y = \infty \quad \text{and all} \quad x > 0 \\ T &= T_w \quad \text{at} \quad y = 0 \quad \text{and all} \quad x > 0. \end{aligned}$$

In accordance with Schmidt's method [21], the derivatives may be replaced by their finite difference approximations based on the notation of Fig. 27.

$$\left.\begin{aligned} \frac{\partial T}{\partial x} &= \frac{T_{m+1,n}-T_{m,n}}{\Delta x} \\ \left.\frac{\partial T}{\partial y}\right|_{m,n} &= \frac{T_{m,n+1}-T_{m,n-1}}{2\Delta y} \\ \left.\frac{\partial k_t}{\partial y}\right|_{m,n} &= \frac{k_{t\,m,n+1}-k_{t\,m,n-1}}{2\Delta y} \\ \left.\frac{\partial^2 T}{\partial y^2}\right|_{m,n} &= \frac{T_{m,n+1}+T_{m,n-1}-2T_{m,n}}{(\Delta y)^2}. \end{aligned}\right\} \tag{6}$$

At any station $m+1$ the only unknown is the temperature T_{m+1}. Therefore equations (6) may be substituted into equation (5) to solve for $T_{m+1,n}$ with respect to temperature, velocity and eddy conductivity at $m, n+1, m, n$ and $m, n-1$. In the same way $T_{m+1,n+1}$ may be determined, and so on.

The finite difference solution will be a good approximation to the exact solution for the temperature distribution at $m+1$ if the stability criterion notably

$$\frac{(k+k_t)}{\rho C_p u}\frac{\Delta x}{(\Delta y)^2}\leqslant\tfrac{1}{2}$$

is maintained.

The heat-transfer rate at the wall can be determined by calculating the first derivative of the temperature profile at the wall using some suitable finite difference formula, for example

$$\left.\frac{\partial T}{\partial y}\right|_{y=0}=\{2\,T_{m,n+2}-9T_{m,n+1}+18T_{m,n}-11T_{m,n-1}\}/6\,\Delta y. \tag{7}$$

From this the local Stanton number

$$St=\frac{-k(\partial T/\partial y)|_{y=0}}{\rho C_p U\,(T_w-T_\infty)} \tag{8}$$

is readily determined.

2. *Implicit method*

Crank and Nicholson [22] suggested that any variable δ may be written in terms of its values at stations m and $m + 1$ (Fig. 27) such that

$$\delta = \theta\delta_{m+1}, \theta\delta_{m+1.n} + (1 - \theta)\delta_{m.n} \tag{9}$$

where θ is a weighting factor, $0 \leqslant \theta \leqslant 1$. The various terms in equation (5) can then be expressed in finite difference form in the following manner.

$$\begin{aligned}
u &= \theta U_{m+1,n} + (1 - \theta)U_{m,n} \\
\frac{\partial T}{\partial x} &= \frac{T_{m+1,n} - T_{m,n}}{\Delta x} \\
\frac{\partial T}{\partial y} &= \theta\left\{\frac{T_{m+1,n+1} - T_{m+1,n-1}}{2\Delta y}\right\} + (1 - \theta)\left\{\frac{T_{m,n+1} - T_{m,n-1}}{2\Delta y}\right\} \\
\frac{\partial^2 T}{\partial y^2} &= \theta\left\{\frac{T_{m+1,n+1} + T_{m+1,n-1} - 2T_{m+1,n}}{(\Delta y)^2}\right\} + (1 - \theta)\left\{\frac{T_{m,n+1} + T_{m,n-1} - 2T_{m,n}}{(\Delta y)^2}\right\}.
\end{aligned} \tag{10}$$

The finite difference expressions (10) when substituted into equation (5) give an equation in three

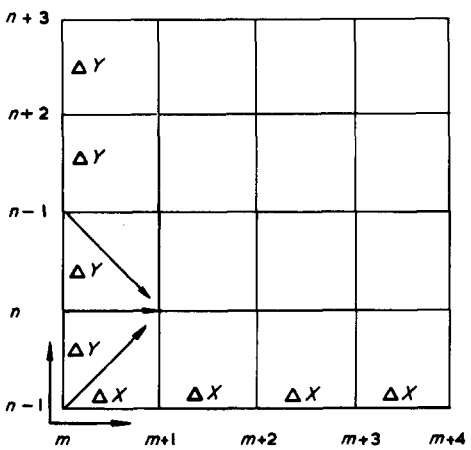

FIG. 27. Grid for finite difference scheme.

unknowns, namely the temperature $T_{m+1,n+1}$ $T_{m+1,n}$ and $T_{m+1,n-1}$. The calculation procedure is started at $y = y(n)$ and is carried out to some boundary $y = y(N)$. This results in a set of $N - n$ equations in $N - n + 2$ unknowns of the form

$$A_{n-1}\, T_{m+1,n-1} + A_n\, T_{m+1,n} + A_{n+1}\, T_{m+1,n+1} = G_n \tag{11}$$

with the boundary conditions

1. at the wall $n = 1$, $T_{m+1,n-1} = T_w$.
   Therefore $A_1 T_{m+1,1} + A_2 T_{m+1,2} = G_1 - A_0 T_w$;
2. at outer boundary $n = N$, $T_{m+1,N+1} = T_\infty$.
   Therefore $A_{N-1}\, T_{m+1,N-1} + A_N T_{m+1,N} = G_N - A_{N+1}\, T_\infty$.

The set of equations when written in matrix form are:

$$\begin{bmatrix} A_1 & A_2 & 0 & 0 \ldots\ldots 0 & 0 & 0 \\ A_1 & A_2 & A_3 & 0 \ldots\ldots 0 & 0 & 0 \\ 0 & A_2 & A_3 & A_4 \ldots\ldots 0 & 0 & 0 \\ \cdot & \cdot & \cdot & \cdot \quad \cdot \quad \cdot & \cdot & \cdot \\ \cdot & \cdot & \cdot & \cdot \quad \cdot \quad \cdot & \cdot & \cdot \\ \cdot & \cdot & \cdot & \cdot \quad \cdot \quad \cdot & \cdot & \cdot \\ 0 \ldots\ldots\ldots\ldots\ldots 0 & A_{N-2} & A_{N-1} & A_N \\ 0 \ldots\ldots\ldots\ldots\ldots 0 & & A_{N-1} & A_N \end{bmatrix} \begin{bmatrix} T_1 \\ T_2 \\ T_3 \\ \cdot \\ \cdot \\ \cdot \\ T_{N-1} \\ T_N \end{bmatrix} = \begin{bmatrix} G_1 - A_0 T_w \\ G_2 \\ G_3 \\ \cdot \\ \cdot \\ \cdot \\ G_{N-1} \\ G_N - A_{N+1} T_\infty \end{bmatrix} \tag{12}$$

This set of equations may be solved for $T = A^{-1}G$ giving the complete distribution of temperature at station $m + 1$.

The heat-transfer rate and the local Stanton number may be calculated as before using equations (7) and (8).

It should be noted that if $\theta = 0$, then equation (5) takes the previously discussed explicit form. In particular if $0 \leqslant \theta \leqslant \frac{1}{2}$ then the method is subject to the general stability condition

$$P \frac{\Delta x}{(\Delta y)^2} \leqslant \frac{1}{2(1 - 2\theta)}.$$

For $\theta \geqslant \frac{1}{2}$ the method should be unconditionally stable and thus any x-step-length may be used. The solution may not converge towards the exact solution, however, if initially too large an x-step is taken, but once the integration is in progress the x-step may be appreciably enlarged.

Crank and Nicholson suggest that $\theta = \frac{1}{2}$ is the appropriate value, but at a recent informal conference on numerical analysis (N.P.L. Teddington, September 1965) it was noted by several investigators that $\theta = \frac{1}{2}$ may produce a cyclic instability in the solution, and that the use of some value of $\theta > \frac{1}{2}$ is advisable.

Résumé—Une nouvelle méthode a été exposée pour calculer le transport de chaleur dans la couche limite turbulente à propriétés constantes avec des distributions arbitraires de température pariétale et de vitesse à l'extérieur de la couche limite. Le processus est décrit ci-dessous.

Le développement de la couche limite est calculé par l'une ou l'autre des méthodes disponibles habituellement et, à partir des valeurs calculées de H et de θ, les profils de vitesse
famille convenable à deux paramètres. Lorsque la distribution de vitesse dans la couche limite est entièrement déterminée, les profils de contrainte tangentielle sont obtenus en appliquant l'équation du mouvement, et à partir des profils de contrainte tangentielle et de vitesse moyenne, les profils corespondants de viscosité effective s'ensuivent facilement.

L'équation du transport de chaleur peut alors, grâce à une hypothèse vraisemblable pour le nombre de Prandtl turbulent, être résolue directement par un calculateur numérique pour obtenir les profils de température et le transport de chaleur à la paroi.

La méthode a été appliquée pour des gradients de pression nuls ou contraires avec un échelon de température pariétale après une longueur d'entrée non chauffée. Les profils de température ont une forme convenable et présentent une région de similitude approchée au voisinage de la paroi comme ce qui a été observé expérimentalement par ailleurs. On remarquera qu'avec un gradient de pression contraire le transport de chaleur diminue beaucoup moins rapidement que le frottement pariétal lorsqu'on s'approche du décollement.

Zussammenfassung—Zur Berechnung des Wärmeübergangs bei turbulenter Grenzschicht mit konstanten Stoffwerten und beliebiger Verteilung von Wandtemperatur und Strömungsgeschwindigkeit wurde eine neue Methode entwickelt.

Das Verfahren ist folgendes: Die Ausbildung der Grenzschicht wird nach der einen oder anderen gegenwärtig verfügbaren Methode berechnet und mit den berechneten Werten von H und θ werden mit Hilfe einer geeigneten Zweiparameter-Gruppe Geschwindigkeitsprofile bestimmt. Mit der für die Grenzschicht vollständig bestimmten Geschwindigkeitsverteilung werden aus der Bewegungsgleichung die Schubspannungsprofile erhalten und aus diesen, zusammen mit der mittleren Geschwindigkeit ergeben sich die entsprechenden Profile der wirksamen Zähigkeit.

Mit einer einleuchtenden Annahme für die turbulente Prantl-Zahl kann die Wärmeübergangsgleichung auf einer Digitalrechenmaschine direkt gelöst werden um Temperaturprofile und den Wärmeübergang an der Wand zu bestimmen.

Die Methode wurde angewandt auf Druckgradienten von Null und solche im Gegensinn für einen Temperatursprung in der Wand, der einer unbeheizten Einlaufstrecke folgt. Die Temperaturprofile zeigen einen Bereich angenäherter Ähnlichkeit in Wandnähe, was schon anderswo experimentell festgestellt wurde. Es ist bemerkenswert, dass für gegensinnigen Druckgradienten bei Annäherung an den Ablösungspunkt der Wärmeübergang wesentlich langsamer abfällt als die Wandreibung.

Аннотация—Разработан новый метод расчета теплообмена в турбулентном пограничном слое с постоянными свойствами при произвольном распределении температуры стенки и скорости течения. Метод состоит в следующем.

Сначала с помощью какого-нибудь известного метода рассчитываем развитие пограничного слоя, а затем полученные величины H и θ используем для определения профиля скорости из семейства кривых для двух параметров. Имея распределение скорости в пограничном слое, из уравнения движения получаем профили напряжения трения, а затем по полученным распределениям напряжения трения и средней скорости легко находим эффективную вязкость.

Сделав соответствующие допущения относительно турбулентного числа Прандтля, можно решить уравнение теплообмена непосредственно на цифровой вычислительной машине и получить распределение температуры и данные о теплообмене стенки.

Этот метод применяется при нулевых и отрицательных градиентах давления и ступенчатом изменении температуры стенки за начальным необогреваемым участком. Можно заметить, что при отрицательном градиенте давления по мере приближения к области отрыва течения интенсивность теплообмена снижается много медленнее, чем поверхностное трение.